Journal of Membrane Science 360 (2010) 1–8

Contents lists available at ScienceDirect

Journal of Membrane Science

journal homepage: www.elsevier.com/locate/memsci

Analytic formulae for the design of reactive polymer blend barrier materials

S. Carranza, D.R. Paul, R.T. Bonnecaze *

Department of Chemical Engineering, The University of Texas at Austin, 1 University Station CO400, Austin, TX 78712, United States

ARTICLE INFO

Article history:
Received 17 October 2009
Received in revised form 13 April 2010
Accepted 21 April 2010
Available online 29 April 2010

Keywords:
Reactive membranes
Packaging
Oxygen scavenging

ABSTRACT

Reactive particles that scavenge an undesirable permeate can be incorporated into thin plastic films to make high performance composite barriers used as packaging materials. A multiscale model is presented with analytic solutions to the resulting equations to describe blends of non-spherical particles in the limiting cases of fast and slow reaction rates. These analytic design formulae include predictions for the permeate flux, time lag and kill time. In particular a quasi-steady permeate flux is quantified, which is observed at early times when most reactive sites are still available. This flux can lead to significant leakage of the mobile species well before the time lag, and it is proposed as a critical figure of merit for the design of reactive barrier materials. The equation for the quasi-steady flux is valid for reactive particles of any shape and requires only knowledge of average area to volume ratio for the particles within the blend in the limit of fast reactions. The time lag is also shown to be valid for any polymer blends, irrespective of particle geometry, aspect ratio or reaction mechanism within the particle. The ranges of validity of the design formulae are found to be broad based on comparisons with numerical solutions of the model.

1. Introduction

Polymers are widely used as packaging materials that provide chemically tunable barrier properties combined with good mechanical properties and low cost. New polymer barrier materials that react or absorb undesirable permeates are being developed for products that are highly sensitive to oxygen or moisture, such as organic light emitting diodes (OLEDs) for flexible displays [1–3]. The characterization and validation of such reactive polymer materials is challenging because they would provide barriers with lifetimes on the order of several years. In practice experiments for characterization would be done on much shorter time scales, and thus models are needed to extrapolate to long times to predict barrier performance. The main purpose of this paper is to develop such models for polymer blends.

Oxygen scavenging polymers (OSPs), like polybutadiene, readily oxidize [4–10]. However, scavenging polymers typically lack adequate structural properties so they are usually employed as composites with polymers such as poly(ethylene terephthalate) (PET) and polystyrene (PS). Polymer blends [11] and multilayer composites [12–17] are two possible configurations of interest. Single layer reactive membranes have been modeled as homogeneous systems [18–25], including the case of reactive particles uniformly dispersed in an inert media. A recent paper by Ferrari et al. [11] presented a multiscale mathematical model describing the transport of oxygen in a blend of spherical OSP particles within an inert polymer matrix. The system of non-linear partial differential equations was solved numerically over a wide parameter space relevant to packaging applications.

This paper significantly extends the methodology developed by Carranza et al. [26] for homogeneous reactive membranes to derive design formulae for polymer blends. It is also shown that this analytical approach can be easily adapted for blends to the practically important case of non-spherical particles. Furthermore, the methodology is demonstrated to accommodate variations in the kinetic model within the reactive particle, and in fact the functional forms of the design equations obtained by asymptotic analysis are independent of the details of the reactive term in the model equations. In particular the limits of fast and slow reactions within the particles are considered here. The derivation of analytical design equations based on approximate solutions of the non-linear model eliminates the need for lengthy simulations and provide clear relationships between critical design parameters and the physical and chemical properties of the polymer blend. In addition, extraction of parameters, such as diffusion and reaction coefficients, and sensitivity analyses are made easier with analytical models.

The results in this paper will be developed in the context of oxygen scavenging but in fact are generally applicable to any reactive permeate and barrier system. Three regimes for the flux of oxygen were observed in the numerical solutions of the multiscale model. At early times, an initial quasi-steady-state flux occurs. This leakage flux, though much smaller than that at true steady state when all the scavengers have been consumed, is likely the most critical characteristic of such barrier materials. At intermediate times, the initial

* Corresponding author. Tel.: +1 512 471 1497; fax: +1 512 471 7060.
E-mail address: rtb@che.utexas.edu (R.T. Bonnecaze).

0376-7388/$ – see front matter © 2010 Elsevier B.V. All rights reserved.
doi:10.1016/j.memsci.2010.04.029

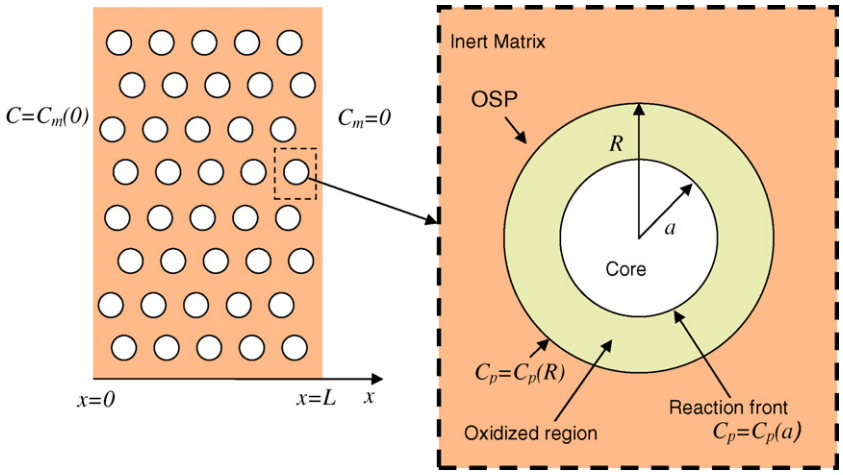

Fig. 1. Schematic illustration of the polymer blend film and a particle in the limit of fast reaction.

plateau gives way to a transient regime with increased oxygen flux, leading to the final regime, characterized by the time lag, when the flux approaches its steady-state value. Analytical estimates for the initial flux plateau, for the intermediate transient flux, the time lag and kill time are presented along with their ranges of validity. The extent and nature of the dependence of each regime on the particle geometry and reactivity is discussed.

2. Model description

Consider a membrane composed of reactive particles in an inert polymer matrix, as illustrated schematically in Fig. 1. The matrix is typically an inert polymer with good mechanical properties, such as poly(ethylene terephthalate) (PET) or polystyrene (PS), while the particles are oxygen scavenging polymers (OSPs) such as polybutadiene (PB). As the matrix is inert, the reaction is confined to the scavenging particles. The particles and the matrix are assumed initially devoid of oxygen. A transport model at the particle-scale is first developed and then used to develop a multiscale transport model in a film of the blend.

2.1. Particle model

The reactive sites within each particle are immobilized and are consumed as reaction progresses. Oxygen transport through the particle obeys Fick's law. Initially, the particles are devoid of oxygen and all reactive sites are available. The material balances, initial and boundary conditions for oxygen and the reactive materials within a spherical particle, for example, are given by

$$\frac{\partial C_p}{\partial t} = \frac{D_p}{r^2}\frac{\partial}{\partial r}\left(r^2\frac{\partial C_p}{\partial r}\right) - k_R n C_p, \tag{1}$$

$$\frac{\partial n}{\partial t} = -\hat{\nu}\, k_R\, n\, C_p, \tag{2}$$

$$\text{I.C.}: \; C_p(r, t=0) = 0, \quad n(r, t=0) = n_0,$$
$$\text{B.C.}: \; \left.\frac{\partial C_p}{\partial r}\right|_{r=0} = 0, \quad C_p(r=R, t) = \frac{C_m}{H}, \tag{3}$$

where C_p is the oxygen concentration within the OSP particle, t is time, r is the radial position in spherical coordinates, D_p is the oxygen diffusion coefficient within the particle, k_R is the bulk reaction rate constant for reactive particle, n is the concentration of reactive sites, $\hat{\nu}$ is the stoichiometric constant relating moles of oxygen to moles of reactive sites, R is the radius of the OSP particle, C_m is the concentration of oxygen in the inert matrix, $H = S_m/S_p$ is the partition coefficient relating the solubility of oxygen in the matrix S_m to the solubility of oxygen oxidized OSP S_p, and n_0 is initial concentration of reactive sites. We will now consider the limiting cases of very fast reaction and very slow reaction.

2.1.1. Reaction is much faster than diffusion

Do [27] has shown that for cases where reaction is much faster than diffusion within the particle, i.e., the Thiele modulus $\Phi_p = (R^2 k_R n_0/D_p)^{1/2} \gg 1$, the shrinking core model is valid. In the shrinking core model the reaction progresses as a moving front, consuming the immobilized sites behind the front, and leaving an unreacted shrinking core ahead of the front. The pseudo-steady-state concentration at the particle's moving front and the rate of change of the core radius are thus given by [11]:

$$C_p(a) = \frac{C_m}{H}\left(1 + \frac{k_p a^2}{D_p R}\left(\frac{R}{a} - 1\right)\right)^{-1}, \tag{4}$$

$$\frac{\partial a}{\partial t} = -\frac{\hat{\nu}\, k_p}{n_0}\frac{C_m}{H}\left(1 + \frac{k_p a^2}{D_p R}\left(\frac{R}{a} - 1\right)\right)^{-1}, \tag{5}$$

where C_m is the oxygen concentration in the inert matrix, k_p is an effective surface rate constant, a is the radius of the reactive core and R is the radius of the OSP particle. The effective surface rate constant in the moving front regime is given by $k_p = \sqrt{D_p k_R n_0}$, as shown in [26]. Sample calculations of the reactive length scale $L_{rxn} = \sqrt{D_p/k_R n_0} = D_p/k_p$, covering the range of values used in numerical calculations of Ferrari et al. [11], are shown in Table 1 (note that in [11] the Damköhler number for the OSP particle is defined by $Da_{OSP} = Rk_P/D_p = \Phi_p$). These indicate the validity of the shrinking core model for much of the practical range of physical parameters. However, as it will be discussed in the next sections, the specific form of Eq. (4) is only required for the derivation of the

Table 1
Sample calculations for OSP particles and blend for range of parameters used in [11].

	k_p (cm/s)	D_p (cm^2/s)	R (μm)	L_{rxn} (μm)	Φ_p	Φ_b
Base case	8×10^{-5}	2×10^{-9}	2.5	0.25	10	104
Highest k_p	1×10^{-3}	2×10^{-9}	2.5	0.02	125	367
Low k_p	1×10^{-6}	2×10^{-9}	2.5	20	0.1	12
High D_p	8×10^{-5}	2×10^{-8}	2.5	2.5	1	104
Low D_p	8×10^{-5}	2×10^{-10}	2.5	0.03	100	104
High R	8×10^{-5}	2×10^{-9}	5.0	0.25	20	73
Low R	8×10^{-5}	2×10^{-9}	0.5	0.25	2	231

$L_{rxn} = D_p/k_p$, $\Phi_p = Rk_P/D_P$, $\Phi_b = \sqrt{3\phi k_p L^2/D_m R H}$, where $D_m = 5.6\times10^{-9}$ cm^2/s, $H = 1$ and $L = 250$ μm for all cases above.

Table 2
Reactive sites material balance for various particle models.[a].

	Shrinking core $\Phi_p \gg 1$	Homogeneous $\Phi_p \ll 1$
Sphere	$\tau = V_0/A_0 k_p$, $V_0/A_0 = R/3$	$\tau = 1/k_R\, n_0$
	$f(n/n_0) = \frac{(n/n_0)^{2/3}}{1+\Phi_p((n/n_0)^{1/3}-(n/n_0)^{2/3})}$	$f(n/n_0) = \frac{n}{n_0}$
Cylinder	$\tau = V_0/A_0 k_p$, $V_0/A_0 \cong R/2$	$\tau = 1/k_R\, n_0$
$h_0 \gg R$	$f(n/n_0) = \frac{(n/n_0)^{1/2}}{1+\Phi_p(n/n_0)^{1/2}\ln((n/n_0)^{-1/2})}$	$f(n/n_0) = \frac{n}{n_0}$
Disk	$\tau = V_0/A_0 k_p$, $V_0/A_0 \cong h_0/2$	$\tau = 1/k_R\, n_0$
$h_0 \ll R$	$f(n/n_0) = \frac{1}{1+\Phi_p(1-n/n_0)}$	$f(n/n_0) = \frac{n}{n_0}$

$k_p = \sqrt{D_p\, k_R n_0}$, $\Phi_p = Rk_p/D_p = \sqrt{R^2 k_R n_0/D_p}$

[a] Scavenger material balance is given by Eq. (12), $\frac{\partial n}{\partial t} = -\frac{\hat{\nu}}{\tau}\frac{C_m}{H} f(n/n_0)$.

intermediates times regime, and variations of Eq. (4) can be easily included in the model.

Eq. (5) can be expressed in terms of the concentration of reactive sites n, which is proportional to the particle volume according to the relationship $n/n_0 = V/V_0 = a^3/R^3$, where n_0 is the initial concentration of reactive sites, V_0 is the initial scavenger particle volume and V is the volume of the unreacted core. Thus, the scavenger site concentration equation and initial condition are given by

$$\frac{\partial n}{\partial t} = -\frac{\hat{\nu}\, k_p A C_p}{V_0} = -\hat{\nu}\frac{3k_p}{R}\frac{C_m}{H}\frac{(n/n_0)^{2/3}}{1+\Phi_p((n/n_0)^{1/3}-(n/n_0)^{2/3})}, \quad (6)$$

$$\text{I.C.}: n(t=0) = n_0, \quad (7)$$

where $A = 4\pi a^2$ is the particle surface area at the moving front, $V_0 = 4\pi R^3/3$ is the initial volume of the particle and $\Phi_p = Rk_P/D_P$ is the Thiele modulus for the particle, expressed in terms of the effective reactive rate constant k_p. Equations similar to Eq. (6) can be derived for shapes other than spheres and are listed in Table 2.

2.1.2. Reaction is much slower than diffusion

When reaction is much slower than diffusion, i.e., $\Phi_p \ll 1$, then the concentration is uniform within the particle and the reactive sites are consumed uniformly over time [28]. Eqs. (1) and (2) and the initial conditions reduce to

$$C_p = \frac{C_m}{H}, \quad (8)$$

$$\frac{\partial n}{\partial t} = -\hat{\nu}\, k_R \frac{C_m}{H} n, \quad (9)$$

$$\text{I.C.}: n(t=0) = n_0. \quad (10)$$

2.2. Transport in the film

Here a model of the transport in the film of the blend is developed based on the particle-scale reaction of oxygen with the scavengers. A schematic of the polymer blend of reactive particles imbedded in an inert matrix is illustrated in Fig. 1. For packaging applications the upstream side is exposed to an infinite source of oxygen at partial pressure $(p_{O_2})_0$ at time $t = 0$. This source is typically air and the downstream side has vanishing oxygen partial pressure. The oxygen concentration at the gas/polymer interface is assumed to obey Henry's law. The particles are assumed to be uniformly distributed, in large enough numbers and small enough compared to the film thickness that average effective properties can be used. The concentration profile over the film takes into account the oxygen consumption in each particle and the number density of particles in the film. The non-linear transport equations in the reactive blend, along with initial and boundary conditions, are given by

$$\frac{\partial C_m}{\partial t} = D_m \frac{\partial^2 C_m}{\partial x^2} + \frac{\phi}{\hat{\nu}}\frac{\partial n}{\partial t}, \quad (11)$$

$$\frac{\partial n}{\partial t} = -\frac{\hat{\nu}}{\tau}\frac{C_m}{H} f(n/n_0), \quad (12)$$

$$\text{I.C.}: C_m(x, t=0) = 0, \quad n(x, t=0) = n_0, \quad (13)$$

$$\text{B.C.}: C_m(0) \equiv C_m(x=0, t) = S_m p_{O_2}, \quad C_m(L) \equiv C_m(x=L, t) = 0. \quad (14)$$

where D_m is the oxygen diffusion coefficient of the inert matrix and ϕ is the volume fraction of OSP in polymer blend. The characteristic time τ and the generic function of reactive sites concentration $f(n/n_0)$ depend on the reactive model chosen for the particle. For spherical particles in the limit of $\Phi_p \gg 1$, $\tau = R/3k_p$ and $f(n/n_0) = (n/n_0)^{2/3}/(1+\Phi_p((n/n_0)^{1/3}-(n/n_0)^{2/3}))$, recovering Eq. (6). In the limit of $\Phi_p \ll 1$, $\tau = 1/k_R\, n_0$ and $f(n/n_0) = n/n_0$, recovering Eq. (9). Expressions for τ and $f(n/n_0)$ for the two different models of particle-scale and particle shapes are given in Table 2. Note that Eq. (12) is the generic form of the material balance for reactive sites, which applies to both the homogeneous (slow reaction) and shrinking core (fast reaction) models of particles of any shape.

The oxygen flux and the total amount of oxygen permeated are quantities of interest derived from the solution of Eqs. (11)–(14). The downstream flux J at time t is given by

$$J\Big|_{x=L} = -D_m \frac{\partial C}{\partial x}\Big|_{x=L}, \quad (15)$$

and the total oxygen permeated through the membrane Q_t at time t is given by

$$Q_t = \int_0^t J|_{x=L}\, dt. \quad (16)$$

Numerical solutions of Eqs. (11)–(14) reveal three regimes of interest for the downstream flux (Fig. 2), as has been shown by Ferrari et al. [11]. The early time regime is characterized by a fast rise of the flux, followed by a flux plateau. This quasi-steady plateau eventually gives way to a second regime of rising oxygen flux. The third regime occurs when all the reactive sites have been consumed, and the flux reaches its final steady-state value. Note that the characteristic times for each regime is independent of Φ_p, as shown in Fig. 2.

The regimes observed in the transient downstream flux can be mapped to the concentration profiles, as illustrated in Fig. 3. The early time regime occurs before significant consumption of reactive sites. Most sites are still available, except for the region very close to the upstream boundary. The uptake of oxygen in this regime can be approximated by a simpler first-order reaction, as will be discussed in the next section. For intermediate times, the concentration profiles can be divided into three zones. The first zone is predominantly diffusive, characterized by a linear oxygen concentration profile, with all the reactive sites consumed. The second zone shows a non-linear decay in the oxygen concentration due to reaction, coupled with a gradual change in reactive sites concentration. In the third zone, most reactive sites are still available, and the oxygen concentration is vanishingly small, which is consistent with the downstream boundary condition. A moving front develops during this regime, leading to the analysis described in Appendix A to develop predictive equations for this regime. Note that this is a front moving through the film and not to be confused with the moving front within the reactive particle illustrated in Fig. 1. Finally, the third regime occurs when all the reactive sites have been consumed, and the concentration profile becomes linear over the whole film. This regime is characterized by the time lag, when the flux approaches its steady-state value.

The three regimes illustrated in Figs. 2 and 3 are observed for reactive transport in reactive polymer blends as well as homogeneous reactive membranes. The analytical solutions for these three

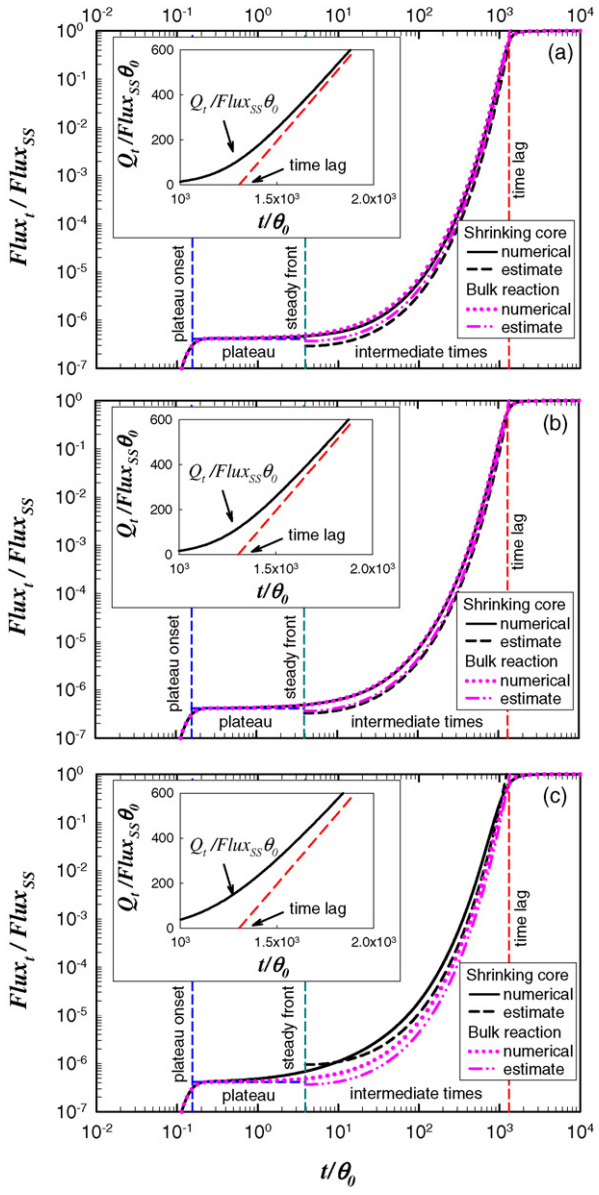

Fig. 2. Comparison of numerical solution and analytical estimates for the three regimes relevant to analysis of dimensionless downstream oxygen flux for $\nu = 0.0023$, $\Phi_b = 18$ and (a) $\Phi_p = 0.125$, (b) $\Phi_p = 1.25$ and (c) $\Phi_p = 12.5$. Solutions based on shrinking core particle model (solid line = numerical solution, dashed line = prediction) and the bulk reaction particle model (dotted line = numerical solution, dash-dot = prediction) are compared. The initial flux plateau (horizontal dashed line) is the same for both models and matches closely the numerical solution. Inset shows the time lag as determined from the numerical solution, using the asymptote as $Q_{t\to\infty}$.

regimes are derived for polymer blends in the next sections, following the framework described in Carranza et al. [26]. Table 3 summarizes the approximate times for each time region in terms of the physical parameters of polymer blends for oxygen scavenging. Similar analysis could be extended to blends targeting other species, e.g. water, by modifying the scavenging behavior accordingly.

3. Analysis of early times to estimate initial leakage flux plateau

At early times, most of the scavenger sites remain unreacted, except those very close to the upstream boundary, as illustrated in Fig. 3. Therefore, the concentration of reactive sites n can be approximated by the initial concentration of reactive sites n_0. The oxygen flux in the plateau region of interest is also quasi-steady, and thus, the oxygen transport equation and boundary conditions become

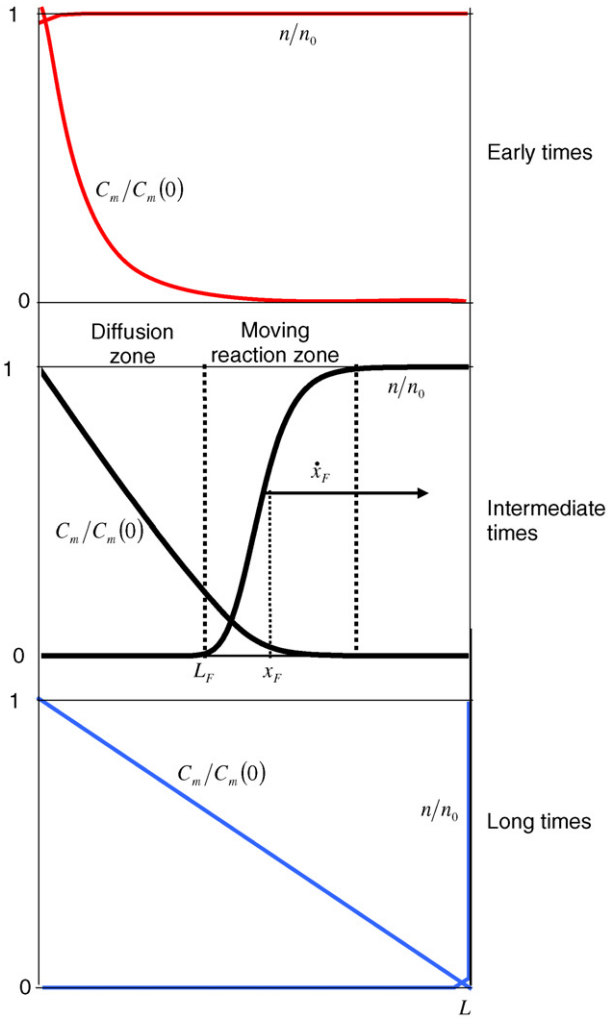

Fig. 3. Concentration profiles for early, intermediate and long times.

$$\frac{d^2C_m}{dx^2} - \frac{\phi}{\tau}\frac{C_m}{H} = 0, \tag{17}$$

$$\text{B.C.}: \quad C_m(0) \equiv C_m(x=0,t) = S_m p_{O_2}, \qquad C_m(L) \equiv C_m(x=L,t) = 0. \tag{18}$$

Table 3
Analytical predictions of dimensionless flux for early, intermediate and long times for a reactive polymer blend.

Time interval	Dimensional equations
Early times[a]	$J\|_{x=L} = 2J_{SS}\Phi_b\, e^{-\Phi_b}$
$t_{onset} \le t \le t_{SF}$	$t_{onset} = \tau((\Phi_b - 1)H/2\phi)$
Intermediate times	$J\|_{x=L} = bJ_{SS}(L/x_F)\, e^{-\Phi_b(1-x_F/L)}$, $x_F = \sqrt{2\,\nu\, D_m\, t}$
$t_{SF} \le t \le \theta$	$t_{SF} = H\tau/2\nu\phi$
Long times	$J\|_{x=L} \to J_{SS} = C_m(0)D_m/L$
$t > \theta$	$\theta = \theta_0(1+3/\nu)$

$\Phi_b = \sqrt{\phi L^2/D_m\tau H}$, $\Phi_p = \sqrt{R^2 k_R\, n_0/D_p}$, $\nu = \hat{\nu}\, C_m(0)/\phi n_0$, $\theta_0 = L^2/6D_m$.
$\tau = 1/k_R\, n_0$ for $\Phi_p \ll 1$, $\tau = V_0/A_0 k_p$ for $\Phi_p \gg 1$.
[a] $J|_{x=L} \cong 0$ for $t < t_{onset}$.

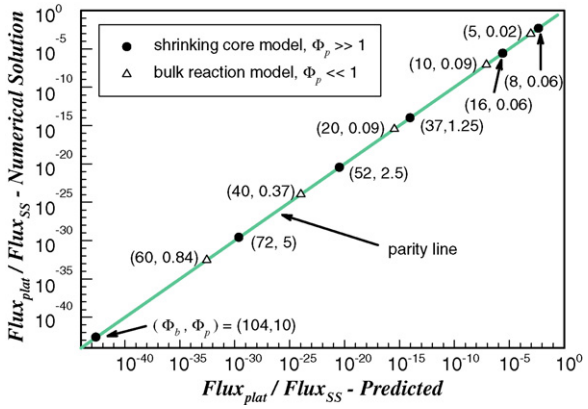

Fig. 4. Parity chart for flux plateau comparing numerical solution and analytical prediction for various Φ_b and Φ_p. The values in parenthesis give Φ_b and Φ_p, respectively, for each data point.

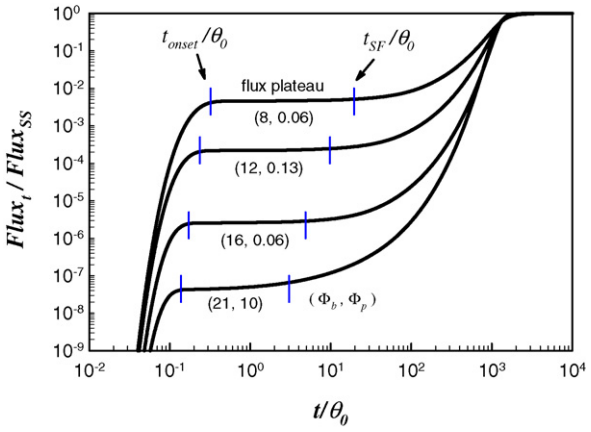

Fig. 5. Dimensionless downstream oxygen flux for $\nu = 0.0023$ and various Φ_b and Φ_p. The values in parenthesis give Φ_b and Φ_p, respectively, for each case. The plateau flux increases with decreasing Φ_b, as predicted by Eq. (21). The initial plateau region is bound by the plateau onset t_{onset} and t_{SF}, as predicted by Eqs. (22) and (23)., respectively.

This equation, along with the boundary conditions can be easily solved to show that

$$C_m = -C_m(0)\frac{\cosh(\alpha L)}{\sinh(\alpha L)}\sinh(\alpha x) + C_m(0)\cosh(\alpha x), \tag{19}$$

where $\alpha = \sqrt{\phi/\tau H}$. Using Eq. (15) for the downstream flux with Eq. (19) for oxygen concentration gives the following expression for the flux:

$$J\big|_{x=L} = \alpha L J_{SS}/\sinh(\alpha L), \quad \text{or} \quad J\big|_{x=L} \sim 2\alpha L J_{SS} e^{-\alpha L} \quad \text{for} \quad \alpha L \gg 1, \tag{20}$$

where J_{SS} is the steady-state oxygen flux $Flux_{SS} = J_{SS} = C_m(0)D_m/L$. Solovyov and Goldman [24] derived a similar equation for the flux to describe a system with a large excess of reactive sites, as part of their modified moving front model. Here this model is used to describe the flux in the early time regime.

This equation can be expressed in terms of the effective Thiele modulus for the film of the polymer blend $\Phi_b = \sqrt{\phi L^2/D_m H\tau}$, i.e., the ratio of the length scale of diffusion through the film and the length scale of reaction within the particle so that

$$Flux_{plat} = J|_{x=L} = 2J_{SS}\Phi_b\, e^{-\Phi_b}, \tag{21}$$

which is valid for $\Phi_b \gg 1$. This algebraic expression predicts the initial flux plateau using physical properties that can be measured experimentally. Note that in the limit of $\Phi_p \ll 1$, $\tau = 1/k_R n_0$ as shown in Table 2, thus making Eq. (21) independent of particle shape or surface area. In the limit of $\Phi_p \gg 1$, $\tau = V_0/A_0 k_p$ in general again regardless of particle shape as shown in Table 2, and thus $\Phi_b = \sqrt{\phi A_0 k_p L^2/V_0 D_m H}$. Therefore, the flux given by Eq. (21) is independent of particle shape and depends only on the specific area A_0/V_0 in the limit of $\Phi_p \gg 1$. In systems where particle shape cannot be described by simple geometries, A_0/V_0 can be determined by analyzing images, e.g., by transmission electron microscopy, using the principles of stereology [29,30]. Eq. (21) is identical in functional form in the limit of fast and slow reactions within the particles. Indeed the existence of the quasi-steady plateau flux is independent of the details of the reaction within the particle because at early times all the scavenging sites are essentially accessible.

The initial plateau estimate of Eq. (21) was compared to the values obtained by numerical solutions of the polymer blend model equations and boundary conditions given by Eqs. (11)–(14) for both fast and slow reactions. The prediction is in excellent agreement with the numerical solutions for all the cases computed, as illustrated in Fig. 2 and the parity plot of Fig. 4. The plateau flux decreases with increasing $\Phi_b = \sqrt{\phi L^2/D_m H\tau}$, as illustrated in Fig. 5. The plateau flux is proportional to the steady-state flux $J_{SS} = C_m(0)D_m/L$, and consequently to the upstream oxygen concentration $C_m(0)$. Increasing D_m increases J_{SS} and decreases Φ_b, leading to an increase in the initial flux plateau. Conversely, increasing L decreases J_{SS} and increases Φ_b, leading to a decrease in the initial flux plateau. The increase in the flux due to increasing $C_m(0)$ or D_m is expected, since the former causes more oxygen to be available, while the later enables fast transport of oxygen through the film, which leads to greater leakage through the film. Likewise, the decrease due to higher L is also expected, since for thicker films, the diffusion time is longer, allowing the reaction to occur and, thus, reducing the amount of oxygen breakthrough at early times.

The onset of the initial plateau t_{onset} can be derived by recognizing that the transient can be modeled as an unsteady first-order reaction diffusion problem. This t_{onset} is the time lag for an equivalent first-order reactive membrane, given by [26]:

$$t_{onset} = \tau\frac{\Phi_b\coth(\Phi_b) - 1}{2\phi/H}, \quad \text{or} \quad t_{onset} \cong \tau\frac{\Phi_b - 1}{2\phi/H} \quad \text{for} \quad \Phi_b \gg 1. \tag{22}$$

Note that the second approximate expression for the onset time retains the constant 1 in the numerator because it is found to be a good approximation for Φ_b as low as 2 or 3.

The initial plateau regime eventually transitions to a fast rise in the downstream oxygen flux, in a transient regime described in the next section. The transition between these two regimes occurs at t_{SF}, the time a steady front has been established. Following the steps in [26], this time can be estimated by comparing the consumption of reactive sites within the front volume with the influx of oxygen into the front volume, and is given by

$$t_{SF} = \tau\frac{H}{2\nu\phi}, \tag{23}$$

where $\nu = \hat{\nu}C_m(0)/\phi n_0$ is the ratio between dissolved oxygen and reactive capacity. When the onset of the initial plateau $t_{onset} = t_{SF}\,\nu(\Phi_b - 1)$ occurs before the steady front has been established, i.e., $0 < \nu(\Phi_b - 1) < 1$, there is a well defined initial plateau regime as the cases shown in Fig. 5, and the transient flux approximation described in the next section is valid.

4. Transient flux regime at intermediate times

To determine the transient flux the specific shape of the particle and the assumed reaction model as embodied by $f(n/n_0)$ must be known. For spherical particles in the limit of $\Phi_p \gg 1$, the concen-

Table 4
Values of b in Eq. (26) for flux estimate for blends of spherical particles with various Φ_p.

$\Phi_p = (R k_P/D_P) = (R^2 k_R n_0/D_p)^{1/2}$	b
Homogeneous film	0.653
0.1	0.514
1	0.581
10	1.54
100	335

tration equations are given by

$$\frac{\partial C_m}{\partial t} = D_m \frac{\partial^2 C_m}{\partial x^2} - \frac{3k_p\phi}{R}\frac{C_m}{H}\frac{(n/n_0)^{2/3}}{1+\Phi_p((n/n_0)^{1/3}-(n/n_0)^{2/3})}, \quad (24)$$

$$\frac{\partial n}{\partial t} = -\hat{\nu}\frac{3k_p}{R}\frac{C_m}{H}\frac{(n/n_0)^{2/3}}{1+\Phi_p((n/n_0)^{1/3}-(n/n_0)^{2/3})}. \quad (25)$$

Solutions in the frame of reference of the moving reaction zone were developed, as shown in Appendix A, giving the algebraic expression for the downstream flux:

$$J\big|_{x=L} = bJ_{SS}\frac{L/x_F}{e^{\Phi_b(1-x_F/L)}}, \quad (26)$$

where $J_{SS} = C_m(0)D_m/L$ is the steady-state oxygen flux and $x_F = \sqrt{2\,\nu\,D_m\,t}$ is the position of the moving front. Values of b in Eq. (26), which are listed in Table 4 for spherical particles and various values of Φ_p, are computed by numerical solutions of the moving front ODEs, as discussed in Appendix A. Note that the functional form of Eq. (26) is valid for a wide range of models, with specific values of b computed for each different model. In the limit of $\Phi_p \ll 1$ the transient result for the homogenous film is recovered where $b = 0.653$ [26]. Fig. 2 compares the numerical solution to the predicted values of the initial flux plateau [Eq. (21)] and the intermediate transient flux [Eq. (26)] using the shrinking core particle model [Eqs. (24) and (25)] and the bulk reaction particle model [Eqs. (11) and (12) where $\tau = 1/k_R n_0$ and $f(n/n_0) = n/n_0$]. The graphs show the results for $\Phi_p = 0.125$, $\Phi_p = 1.25$ and $\Phi_p = 12.5$, where $\nu = 0.0023$ and $\Phi_b = 18$ for all cases. Note that the results for the shrinking core particle model and the bulk reaction particle model are nearly identical for $\Phi_p = 0.125$ and $\Phi_p = 1.25$, therefore both models can be used in this range of Φ_p.

As indicated in Table 3, the transient flux prediction of Eq. (26) is valid between the time a steady front has been established [t_{SF} given by Eq. (23)] to the time before the front has reached the right boundary, i.e., when most of the reactive sites have been consumed. Note that for larger Φ_p (Fig. 2c) the flux increase from the initial plateau flux starts before t_{SF}, resulting in a larger deviation from the predicted values.

5. Figures of merit

The prediction of time lag θ for a reactive polymer blend was derived in Ferrari et al. [11], following a method developed by Frisch [31], and adapted by Siegel and Cussler [18] to estimate the time lag for homogeneous reactive membranes. The expression derived by Ferrari et al. is given by

$$\theta = \theta_0(1 + 3/\nu), \quad (27)$$

where $\theta_0 = L^2/6D_m$ is the diffusion time lag of the inert matrix and $\nu = \hat{\nu}C_m(0)/\phi n_0$ is the ratio between dissolved oxygen and reactive capacity. This algebraic equation for time lag was obtained assuming spherical particles, but is in fact generally valid irrespective of the shapes or sizes of the particles, and irrespective of the specific reaction mechanism within the particles. Note that the time lag depends only on the diffusion time scale through the inert matrix, and the ratio between dissolved oxygen and scavenging capacity of the blend.

The cumulative oxygen permeate Q_t is obtained by the integration of the downstream flux, per Eq. (16), and can be estimated analytically by adding the contributions from the initial plateau regime, see Eq. (21), and the transient regime, see Eq. (26). Thus, the oxygen permeate can be estimated by

$$Q_t = \int_{t_{onset}}^{t_{SF}} J\big|_{x=L}dt + \int_{t_{SF}}^{t} J\big|_{x=L}dt = \frac{2J_{SS}t_{SF}\Phi_b}{e^{\Phi_b}}(1+\nu(1-\Phi_b)+b(e^{\sqrt{t/t_{SF}}}-e)). \quad (28)$$

For times below t_{SF}, the above equation reduces to the first integral, $2J_{SS}\Phi_b e^{-\Phi_b}(t + t_{SF}\nu(1-\Phi_b))$, which is the initial flux plateau multiplied by $t - t_{onset}$. The kill time t_K, i.e., the time when the oxygen permeate reaches a predefined max Q_{max}, proposed as a transient parameter in [22], can be found by solving Eq. (28) for time, giving

$$t_k = t_{SF}\ \ln^2\left[\frac{Q_{\max}e^{\Phi_b}}{2bJ_{SS}t_{SF}\Phi_b} - \frac{1+\nu(1-\Phi_b)}{b} + e\right]. \quad (29)$$

6. Summary and conclusions

The transport equations for a mobile permeate in a blend of reactive particles in an inert matrix have been derived to describe reactive particles of any shape in the limits of fast reaction and slow reaction. The framework developed to derive analytical design formulae for homogeneous reactive membranes [26] has been extended to these reactive polymer blends, illustrating how the approach can be adapted for models with very distinct reactive terms. Equations for flux and characteristic times for the three regimes identified in the numerical solutions have been derived for the polymer blend. It was found that the details of the reaction mechanism within the particles do not affect the functional form of the analytic models and only affect the values of known or easily determined constants in the predictive equations. The technique presented is broadly applicable and can be easily adapted to accommodate other particle-scale reaction models.

For the initial regime, when most reactive particles are still available, the initial plateau flux and plateau onset time t_{onset} can be determined without knowledge of particle shapes, using instead the average area to volume ratio of the reactive particles A_0/V_0, which can be determined by analyzing images using the principles of stereology. Likewise, the characteristic time for the intermediate regime t_{SF}, which marks the end of the initial flux plateau, requires only knowledge of A_0/V_0. One of the critical conclusions of this paper is the generality of Eq. (21) for the prediction of this flux. For many packaging applications, the initial plateau flux is the important design consideration because it characterizes the small but persistent leakage of oxygen through the barrier. Furthermore, the calculations for early times do not require the knowledge of the reaction details within the particle. The value of the downstream flux for intermediate times can be predicted analytically if the particle shape is known. The third regime, when most particles have been consumed, is characterized by the time lag θ and the steady-state flux, which are completely independent of particle shape, area to volume ratios, or details of reaction within each particle.

Traditionally, the time lag, which is independent of reaction rate, has been considered the figure of merit when designing reactive membranes, as it marks the exhaustion of the reactive particles. However, this study suggests that the value of the initial flux plateau, which accounts for both diffusion and reaction rates, along

with its end time t_{SF} are additional parameters to consider when designing packaging materials. For applications where it may be preferable to design a barrier which will remain in the plateau region throughout the life of the product, the end of the useful life may be determined by the beginning of the transient region t_{SF} instead of time lag θ, and the value of the flux plateau can be used to determine the total permeate over the life of the product.

Acknowledgment

This work was supported in part by the National Science Foundation under Grant Number DMR0423914.

Appendix A.

Following Carranza et al. [26], solutions in the frame of reference of the moving reaction zone were developed, with solutions of the form:

$$\frac{n(x,t)}{n_0} = \eta(\xi), \tag{A.1}$$

$$C(x,t) = C_m(0)\sqrt{\frac{H\tau}{t\phi}}G(\xi), \tag{A.2}$$

$$\xi = \frac{x - x_F(t)}{\sqrt{D_m H\tau/\phi}}, \tag{A.3}$$

where $\eta(\xi)$ represents the reactive site in the new frame of reference, $G(\xi)$ is the self-similar oxygen concentration field, $H\tau/\phi$ is the reactive time scale for the blend, $\sqrt{D_m H\tau/\phi}$ is the reactive length scale for the blend. The position of the moving front is given by

$$x_F = \sqrt{2\,\nu D_m\, t}, \tag{A.4}$$

where $\nu = \hat{\nu}\, C_m\,(0)\,/\phi\, n_0$ is the ratio between dissolved oxygen and reactive capacity. The leading order equations for the polymer blend become

$$\frac{d^2\hat{G}}{d\xi^2} - \hat{G}f(\eta) = 0, \tag{A.5}$$

$$\frac{d\eta}{d\xi} - \hat{G}f(\eta) = 0, \tag{A.6}$$

$$\text{B.C.}: \quad \eta(\infty) = 1, \quad \hat{G}(\infty) = 0, \quad \left.\frac{d\hat{G}}{d\xi}\right|_{-\infty} = -1, \tag{A.7}$$

where $\hat{G} = \sqrt{2\nu}G$.

Provided that $f(\eta) \to 1$ as $\xi \to \infty$, the asymptotic solutions of these equations as $\xi \to \infty$ are given by

$$\hat{G} = be^{-\xi}, \quad \eta = 1 - be^{-\xi}. \tag{A.8}$$

Thus, substituting Eq. (A.8) in Eq. (A.2) for concentration in the moving front regime and using Eq. (15) for flux gives Eq. (26), the algebraic expression for the downstream flux. Note that Eq. (26) functional form is valid for any model with the asymptote $f(\eta) \to 1$ as $\xi \to \infty$, regardless of the details of $f(\eta)$. If $f(\eta)$ is known, the values of b may be computed by solving Eqs. (A.5) and (A.6) by the shooting method using Eq. (A.8) as the initial conditions while varying b until the condition for matching the asymptotic solutions of the diffusion zone and the moving reaction zone is satisfied, i.e., $\hat{G}(\xi) = -\xi$ as $\xi \to -\infty$ [26].

Nomenclature

a	radius of the reactive core, cm
A	area of scavenging core, cm^2
A_0	area of scavenging particle, cm^2
b	constant for moving front flux prediction, dimensionless
C_m	O_2 concentration in the film, mol_{O_2}/cm^3
$C_m(0)$	oxygen concentration at the polymer blend film upstream surface $C_m(0) = p_{O_2}S_m$, mol_{O_2}/cm^3
C_p	oxygen concentration in the OSP particle, mol_{O_2}/cm^3 OSP
D_m	oxygen diffusion coefficient of the inert matrix, cm^2/s
D_p	oxygen diffusion coefficient for the oxidized OSP, cm^2/s
$f(n/n_0)$	reactive sites consumption function for a particle
G	variable for moving front analysis, dimensionless $\hat{G} = \sqrt{2\nu}G$
H	partition coefficient, $H = S_m/S_p$
J	oxygen flux, mol/cm^2 s
k_p	reaction rate constant for reactive particle, cm/s
k_R	bulk reaction rate constant for reactive particle, cm^3 OSP/mol_{RS} s
L	thickness of the film, cm
n	concentration of reactive sites, mol_{RS}/cm^3
n_0	initial concentration of reactive sites, mol_{RS}/cm^3
p_{O_2}	oxygen partial pressure, MPa
Q_t	oxygen permeate, mol/cm^2
R	radius of the OSP particle, cm
S_m	solubility coefficient for oxygen in inert matrix, cm^3(STP)/cm^3 MPa
S_p	solubility coefficient for oxygen in the scavenging polymer, cm^3(STP)/cm^3 MPa
t	time, s
t_K	kill time, s
t_{onset}	onset time for the initial flux plateau, s
t_{SF}	time when a steady moving front is established, s
V	volume of reactive core, cm^3
V_0	volume of scavenging particle, cm^3
x	position along film thickness, cm
x_F	moving front position, cm
$\dot{x}_F$	moving front speed, cm/s
$\sim$	denotes dimensionless variables

Greek letters

β	OSP capacity, $\beta = n_0/\hat{\nu}$, mol_{O_2}/cm^3 OSP
θ	time lag, s
θ_0	diffusion time lag of inert polymer, $\theta_0 = L^2/6D_m$, s
ϕ	volume fraction of OSP in polymer blend
Φ_b	effective Thiele modulus for the blend, $\Phi_b = \sqrt{\phi L^2/D_m\tau H}$
Φ_p	Thiele modulus for the OSP particle, $\Phi_p = \sqrt{R^2k_Rn_0/D_p}$ or $\Phi_p = Rk_p/D_p$
η	reactive sites expressed in terms of moving front coordinate
ν	ratio between dissolved oxygen and reactive capacity, $\nu = \hat{\nu}C_m(0)/\phi n_0$
$\hat{\nu}$	stoichiometric coefficient, $mol_{RS}mol_{O_2}$
τ	time scale, $\tau = V_0/A_0k_p$ or $\tau = 1/k_R\,n_0$, s
ξ	moving front coordinate, dimensionless

References

[1] P.E. Burrows, et al., Gas permeation and lifetime tests on polymer-based barrier coatings, Proc. SPIE 4105 (2001) 75–83.
[2] J. Lewis, Material challenge for flexible organic devices, Mater. Today 9 (2006) 38–45.
[3] M.C. Choi, Y. Kim, C.S. Ha, Polymers for flexible displays: from material selection to device applications, Prog. Polym. Sci. 33 (2008) 581–630.
[4] A.V. Tobolsky, D.J. Metz, R.B. Mesrobian, Low temperature autoxidation of hydrocarbons: the phenomenon of maximum rates, J. Am. Chem. Soc. 72 (1950) 1942–1952.
[5] R.G. Bauman, S.H. Maron, Oxidation of polybutadiene. I. Rate of oxidation, J. Polym. Sci. 22 (1956) 1–12.
[6] S.W. Beavan, D. Phillips, Mechanistic studies on the photo-oxidation of commercial poly(butadiene), Eur. Polym. J. 10 (1974) 593–603.
[7] J.F. Rabek, J. Lucki, B. Rånby, Comparative studies of reactions of commercial polymers with molecular oxygen, singlet oxygen, atomic oxygen and ozone-I, Eur. Polym. J. 15 (1979) 1089–1100.
[8] V.B. Ivanov, S.G. Burkova, Y.L. Morozov, V.Y. Shlyapintokh, Kinetics of the chain-propagation and chain-termination reactions in the oxidation of polybutadiene and copolymers of butadiene with styrene, Kinet. Katal. 20/5 (1979) 1330–1333.
[9] C. Adam, J. Lacoste, J. Lemaire, Photo-oxidation of elastomeric materials. Part 1-Photo-oxidation of polybutadienes, Polym. Degrad. Stabil. 24 (1989) 185–200.
[10] M. Piton, A. Rivaton, Photooxidation of polybutadiene at long wavelengths ($\lambda > 300$ nm), Polym. Degrad. Stabil. 53 (1996) 343–359.
[11] M.C. Ferrari, S. Carranza, R.T. Bonnecaze, K.K. Tung, B.D. Freeman, D.R. Paul, Modeling of oxygen scavenging for improved barrier behavior: blend films, J. Membr. Sci. 329 (2009) 183–192.
[12] C.D. Mueller, S. Nazarenko, T. Ebeling, T.L. Schuman, A. Hiltner, E. Baer, Novel structures by microlayer coextrusion—Talc-filled PP, PC/SAN, and HDPE/LLDPE, Polym. Eng. Sci. 37/2 (1997) 355–362.
[13] E.E. Nuxoll, E.L. Cussler, Layered reactive barrier films, J. Membr. Sci. 252 (2005) 29–36.
[14] S.E. Solovyov, A.Y. Goldman, Optimized design of multilayer barrier films incorporating a reactive layer. I. Methodology of ingress analysis, J. Appl. Polym. Sci. 100 (2006) 1940–1951.
[15] S.E. Solovyov, A.Y. Goldman, Optimized design of multilayer barrier films incorporating a reactive layer. II. Solute dynamics in two-layer films, J. Appl. Polym. Sci. 100 (2006) 1952–1965.
[16] S.E. Solovyov, A.Y. Goldman, Optimized design of multilayer barrier films incorporating a reactive layer. III. Case analysis and generalized multilayer solutions, J. Appl. Polym. Sci. 100 (2006) 1966–1977.
[17] S.E. Solovyov, A.Y. Goldman, Mass Transport Reactive Barriers in Packaging, DEStech Publications, Lancaster, PA, 2008.
[18] R.A. Siegel, E.L. Cussler, Reactive barrier membranes: some theoretical observations regarding the time lag and breakthrough curves, J. Membr. Sci. 229 (2004) 33–41.
[19] C. Yang, E.E. Nuxoll, E.L. Cussler, Reactive barrier films, AIChE J. 47/2 (2001) 295–302.
[20] C. Yang, E.L. Cussler, Oxygen barriers that use free radical chemistry, AIChE J. 47/12 (2001) 2725–2732.
[21] N.K. Lape, C. Yang, E.L. Cussler, Flake-filled reactive membranes, J. Membr. Sci. 209 (2002) 271–282.
[22] E.E. Nuxoll, E.L. Cussler, The third parameter in reactive barrier films, AIChE J. 51/2 (2005) 456–463.
[23] S.E. Solovyov, A.Y. Goldman, Theory of transient permeation through reactive barrier films. I. Steady state theory for homogeneous passive and reactive media, Int. J. Polym. Mater. 54 (2005) 71–91.
[24] S.E. Solovyov, A.Y. Goldman, Theory of transient permeation through reactive barrier films. II. Two layer reactive-passive structures with dynamic interface, Int. J. Polym. Mater. 54 (2005) 93–115.
[25] S.E. Solovyov, A.Y. Goldman, Theory of transient permeation through reactive barrier films. III. Solute ingress dynamics and model lag times, Int. J. Polym. Mater. 54 (2005) 117–139.
[26] S. Carranza, D.R. Paul, R.T. Bonnecaze, Design formulae for reactive barrier membranes, Chem. Eng. Sci. 65 (2010) 1151–1158.
[27] D.D. Do, On the validity of the shrinking core model in noncatalytic gas solid reaction, Chem. Eng. Sci. 37/10 (1982) 1477–1481.
[28] O. Levenspiel, Chemical Reaction Engineering, 3rd ed., John Wiley & Sons, New York, 1999.
[29] G. Thomas, M.J. Goringe, Transmission Electron Microscopy of Materials, Wiley, New York, 1979.
[30] J.C. Russ, R.T. Dehoff, Practical Stereology, 2nd ed., Kluwer Academic/Plenum Publishers, New York, 2000.
[31] H.L. Frisch, The time lag in diffusion, J. Phys. Chem. 61 (1957) 93–95.